Applied Mathematics and Mechanics
(English Edition, Vol 24, No 1, Jan 2003)

Published by Shanghai University,
Shanghai, China

Article ID: 0253-4827(2003)01-0001-13

INVESTIGATION OF THE DYNAMIC BEHAVIOR OF TWO COLLINEAR ANTI-PLANE SHEAR CRACKS IN A PIEZOELECTRIC LAYER BONDED TO TWO HALF SPACES BY A NEW METOHD *

ZHOU Zhen-gong (周振功), WANG Biao (王 彪)

(Center for Composite Materials and Electro-Optics Research Center,
Harbin Institute of Technology, Harbin 150001, China)

(Contributed by WANG Biao)

Abstract: *The dynamic behavior of two collinear anti-plane shear cracks in a piezoelectric layer bonded to two half spaces subjected to the harmonic waves is investigated by a new method. The cracks are parallel to the interfaces in the mid-plane of the piezoelectric layer. By using the Fourier transform, the problem can be solved with two pairs of triple integral equations. These equations are solved by using Schmidt's method. This process is quite different from that adopted previously. Numerical examples are provided to show the effect of the geometry of cracks, the frequency of the incident wave, the thickness of the piezoelectric layer and the constants of the materials upon the dynamic stress intensity factor of cracks.*

Key words: Schmidt's method; triple integral equations; piezoelectric materials; dynamic stress intensity factor; cracks;

Chinese Library Classification: O345.51 **Document code**: A

2000 MR Subject Classification: 74R10; 74F15

Introduction

It is well-known that piezoelectric materials produce an electric field when deformed and undergo deformation when subjected to an electric field. The coupling nature of piezoelectric materials has attracted wide applications in electro-mechanical and electric devices, such as electro-mechanical actuators, sensors and structures. When subjected to mechanical and electrical loads in service, these piezoelectric materials can fail prematurely due to defects, e.g., cracks, holds, etc. arising during their manufacture process. Therefore, it is of great importance to study the electro-elastic interaction and fracture behavior of piezoelectric materials. Moreover, it is known that the failure of solids, results from the final propagation of the cracks, and in most

* **Received date**: 2001-07-19; **Revised date**: 2002-07-20

Foundation items: the National Natural Science Foundation of China (10172030); the Key Project of National Natural Science Foundation of China (50232030)

Biography: ZHOU Zhen-gong (1963 -), Professor, Dorctor (E-mail: zhouzhg@hope.hit.edu.cn)

cases, the unstable growth of the crack is brought about by the external dynamic loads. So, the study of the dynamic fracture mechanics of piezoelectric materials is much more important in recent research.

In the theoretical studies of crack problems, several different electric boundary conditions at the crack surfaces have been proposed by numerous researchers[1-14]. For the sake of analytical simplification, the assumption that the crack surfaces are impermeable to electric fields was adopted by some researchers[1-6, 14]. In these models, the assumption of the impermeable cracks refers to the fact that the crack surfaces are free of surface charge and thus the electric displacement vanishes inside the crack. In fact, cracks in piezoelectric materials consist of vacuum, air or some other gas. This requires that the electric fields can propagate through the crack, so the electric displacement component perpendicular to the crack surfaces should be continuous across the crack surfaces. However, due to much simpler treatment from a mathematical point of view, the impermeable crack are still employed extensively in the study of the crack problems of piezoelectric materials[1-4, 14-16]. Recently, the dynamic response of piezoelectric materials and the failure modes have attracted more and more attention from many researchers[15-20]. A finite crack in an infinite piezoelectric material strip under anti-plane dynamic electro-mechanical impact was investigated with the well-established integral transform methodology by Yu and Chen[15]. Axisymmetric vibration of a piezo-composite hollow cylinder was studied by Paul and Nelson[17]. The dynamic representation formulas and fundamental solutions for piezoelectricity had been proposed earlier by Khutoryansky and Sosa[18]. The dynamic response of a cracked dielectric medium in a uniform electric field was studied by Shindo[19]. Narita and Shindo[20] also carried our an analysis of the scattering of anti-plane shear waves by a finite crack in piezoelectric laminates. In particular, control of laminated structures including piezoelectric devices was the subject of research in Refs. [21 - 25]. Many piezoelectric devices comprise both piezoelectric and structural layers, and an understanding of the fracture process of piezoelectric structural systems is of great importance in order to ensure the structural integrity of piezoelectric devices[25, 26]. However, the electro-elastic dynamic behavior of laminated piezoelectric composite structures with two cracks has not been studied despite the fact that many piezoelectric devices are constructed in a laminated form. Accordingly, there is a need to investigate the electro-elastic fracture mechanics analysis of laminated piezoelectric structures.

In the present paper, we consider the anti-plane shear problem for two cracked piezoelectric layers bonded to two half spaces. The two half spaces have similar properties and the piezoelectric laminate is subjected to combined mechanical and electrical loads. The cracks are situated symmetrically and oriented in the direction parallel to the interfaces of the layer. The interaction between two collinear symmetrical cracks subjects to anti-plane shear waves in piezoelectric layer bonded to two half spaces is investigated using a some different approach by a new method, namely Schmidt's method[27]. It is a simple and convenient method for solving this problem. Fourier transform is applied and a mixed boundary value problem is reduced to two pairs of triple integral equations. In solving the triple integral equations, the crack surface displacement and electric potential are expanded in a series of Jacobi polynomials and Schmidt's method[27] is used. This process is quite different from that adopted in Refs. [1 - 13, 15 - 26]. The form of solution is easy to understand. Numerical calculations are carried out for the stress intensity factors.

1 Formulation of the Problem

Consider a piezoelectric layer that is sandwiched between two elastic half planes with an elastic stiffness constant c_{44}^{E}. Quantities in the half spaces will subsequently be designated by superscript E. The piezoelectric material layer of thickness $2h$ contains two cracks of length $1-b$ that are situated in the mid-plane and are parallel to the interfaces, as shown in Fig.1, $2b$ is the distance between the cracks ($2b$ is the distance between the cracks. The piezoelectric boundary-value problem for and anti-plane shear change in the numerical values of the present paper. $a > b > 0$). The piezoelectric boundary-value problem for anti-plane shear is considerably simplified if we consider only the out-of-plane displacement and the in-plane elastic fields. Let ω be the circular frequency of the incident wave. In what follows, the time dependence of all field quantities assumed to be of the form $\exp(-i\omega t)$ will be suppressed but understand. The constitutive equations can be written as

$$\tau_{zk} = C_{44} w_{,k} + e_{15} \phi_{,k} \quad (k = x, y), \tag{1}$$

$$D_k = e_{15} w_{,k} - \varepsilon_{11} \phi_{,k} \quad (k = x, y), \tag{2}$$

$$\tau_{xz}^{E} = c_{44}^{E} w_{,x}^{E}, \qquad \tau_{yz}^{E} = c_{44}^{E} w_{,x}^{E}, \tag{3,4}$$

where τ_{zk}, $D_k(k = x, y)$ are the anti-plane shear stress and in-plane electric displacement, respectively. c_{44}, e_{15}, ε_{11} are the shear modulus, piezoelectric coefficient and dielectric parameter, respectively. w and ϕ are the mechanical displacement and electric potential. τ_{xz}^{E}, τ_{yz}^{E} and w^{E} are the shear stress, and the displacement in the half elastic spaces, respectively. The anti-plane governing equations are[26]

$$c_{44} \nabla^2 w + e_{15} \nabla^2 \phi = \rho \partial^2 w / \partial t^2, \tag{5}$$

$$e_{15} \nabla^2 w - \varepsilon_{11} \nabla^2 \phi = 0, \tag{6}$$

$$\nabla^2 w^{E} = \rho^{E} \partial^2 w^{E} / \partial t^2, \tag{7}$$

where $\nabla^2 = \partial^2/\partial x^2 + \partial^2/\partial y^2$ is the two-dimensional Laplace operator. ρ is the mass density of the piezoelectric materials. ρ^E is the mass density of the elastic materials. Body force, other than inertia, and the free charge are ignored in present work. Because of the assumed symmetry in geometry and loading, it is sufficient to consider the problem for $0 \leqslant x < \infty$, $0 \leqslant y < \infty$ only.

A Fourier transform is applied to Eqs. (5), (6) and (7). Assume that the solutions are

$$w(x, y, t) = \frac{2}{\pi} \int_0^\infty \{A_1(s) \exp[-\gamma_1 y] + A_2(s) \exp[\gamma_1 y]\} \cos(sx) \mathrm{d}s, \tag{8}$$

$$w^{E}(x, y, t) = \frac{2}{\pi} \int_0^\infty A_3(s) \exp[-\gamma_2 y] \cos(sx) \mathrm{d}s, \tag{9}$$

where $\gamma_1 = \sqrt{s^2 - (\omega / c_{SH})^2}$, $c_{SH} = \sqrt{\mu / \rho}$, $\mu = c_{44} + \dfrac{e_{15}^2}{\varepsilon_{11}}$, $\gamma_2 = \sqrt{s^2 - (\omega / (c_{SH}^{E})^2}$, $c_{SH}^{E} = \sqrt{c_{44}^{E} / \rho^{E}}$. $A_1(s)$, $A_2(s)$ and $A_3(s)$ are unknown functions, and a superposed bar indicates the Fourier transform throughout the paper, e.g.,

$$\bar{f}(s) = \int_{-\infty}^{\infty} f(x)\mathrm{e}^{-\mathrm{i}sx}\mathrm{d}x. \tag{10}$$

Inserting Eq.(8) into Eq.(6), it can be assumed

$$\phi(x,y,t) - \frac{e_{15}}{\varepsilon_{11}}w(x,y,t) = \frac{2}{\pi}\int_0^{\infty}[B_1(s)\mathrm{e}^{-sy} + B_2(s)\mathrm{e}^{sy}]\cos(sx)\mathrm{d}s, \tag{11}$$

where $B_1(s)$ and $B_2(s)$ are unknown functions.

As discussion in Refs.[15,19,20], the boundary conditions of the present problem are (In this paper, we just consider the perturbation stress field.)

$$\tau_{yz}(x,0,t) = -\tau_0 \qquad (b \leqslant |x| \leqslant 1), \tag{12}$$

$$D_y(x,0,t) = -D_0 \qquad (b \leqslant |x| \leqslant 1), \tag{13}$$

$$w(x,0,t) = \phi(x,0,t) = 0 \qquad (|x| < b, |x| > 1), \tag{14}$$

$$\tau_{yz}(x,h,t) = \tau_{yz}^{\mathrm{E}}(x,h,t), \tag{15}$$

$$w(x,\pm h,t) = w^{\mathrm{E}}(x,\pm h,t), \tag{16}$$

$$D_y(x,\pm h,t) = 0, \tag{17}$$

$$w(x,y,t) = w^{\mathrm{E}}(x,y,t) = \phi(x,y,t) = 0, \quad \text{for } \sqrt{x^2+y^2} \to \infty. \tag{18}$$

In this paper, the wave is vertically incident and we only consider that τ_0 and D_0 are positive. The boundary conditions can be applied to yield two pairs of triple integral equations:

$$\frac{2}{\pi}\int_0^{\infty} A(s)\cos(sx)\mathrm{d}s = 0 \qquad (0 \leqslant x < b, 1 < x), \tag{19}$$

$$\frac{2}{\pi}\int_0^{\infty} \gamma_1 F_1(s)A(s)\cos(sx)\mathrm{d}s = \frac{1}{\mu}\left(\tau_0 + \frac{e_{15}D_0}{\varepsilon_{11}}\right) \qquad (b \leqslant x \leqslant 1) \tag{20}$$

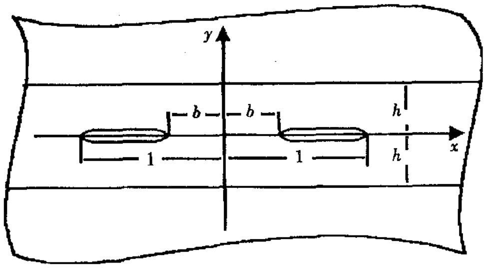

Fig.1 Cracks in a piezoelectric layer under anti-plane shear waves

and

$$\frac{2}{\pi}\int_0^{\infty} B(s)\cos(sx)\mathrm{d}s = 0 \qquad (0 \leqslant x < b, 1 < x), \tag{21}$$

$$\frac{2}{\pi}\int_0^{\infty} sF_1(s)B(s)\cos(sx)\mathrm{d}s = -\frac{D_0}{\varepsilon_{11}} \qquad (b \leqslant x \leqslant 1), \tag{22}$$

where $F_1(s) = \dfrac{1-\mu_3\mathrm{e}^{-2\gamma_1 h}}{1+\mu_3\mathrm{e}^{-2\gamma_1 h}}$, $F_2(s) = \dfrac{1-\mathrm{e}^{-2sh}}{1+\mathrm{e}^{-2sh}}$, $A(s) = (1+\mu_3\mathrm{e}^{-2s_1 h})A_1(s)$,

$A_2(s) = \mu_3\mathrm{e}^{-2\gamma_1 h}A_1(s)$, $B(s) = (1+\mathrm{e}^{-2sh})B_1(s)$, $B_2(s) = \mathrm{e}^{-2sh}B_1(s)$,

$\mu = c_{44} + \dfrac{e_{15}^2}{\varepsilon_{11}}$, $\mu_1 = \gamma_1 - \dfrac{c_{44}^{\mathrm{E}}}{\mu}\gamma_2$, $\mu_2 = \gamma_1 + \dfrac{c_{44}^{\mathrm{E}}}{\mu}\gamma_2$, $\mu_3 = \dfrac{\mu_1}{\mu_2}$.

To determine the unknown functions $A(s)$, $B(s)$, the above two pairs of triple integral

Eqs. (19) - (22) must be solved.

2 Solution of the Triple Integral Equation

For solving two pairs of triple integral equations, the Schmidt's method[27] can be used to solve the triple integral Eqs. (19) - (22). The displacement w and the electric potential ϕ can be represented by the following series:

$$w(x,0,t) = \sum_{n=0}^{\infty} a_n \mathrm{P}_n^{(\frac{1}{2},\frac{1}{2})}\left(\frac{x-\frac{1+b}{2}}{\frac{1-b}{2}}\right)\left(1-\frac{\left(x-\frac{1+b}{2}\right)^2}{\left(\frac{1-b}{2}\right)^2}\right)^{\frac{1}{2}},$$

$$\text{for } b \leqslant x \leqslant 1,\ y = 0, \tag{23}$$

$$w(x,0,t) = 0, \qquad \text{for } x < b,\ x > 1,\ y = 0, \tag{24}$$

$$\phi(x,0,t) = \sum_{n=0}^{\infty} a_n \mathrm{P}_n^{(\frac{1}{2},\frac{1}{2})}\left(\frac{x-\frac{1+b}{2}}{\frac{1-b}{2}}\right)\left(1-\frac{\left(x-\frac{1+b}{2}\right)^2}{\left(\frac{1-b}{2}\right)^2}\right)^{\frac{1}{2}},$$

$$\text{for } b \leqslant x \leqslant 1,\ y = 0, \tag{25}$$

$$\phi(x,0,t) = 0, \qquad \text{for } x < b,\ x > 1,\ y = 0, \tag{26}$$

where a_n and b_n are unknown coefficients to be determined and $\mathrm{P}_n^{(1/2,1/2)}(x)$ is a Jacobi polynomial[28]. The Fourier transformation of Eqs. (23) and (25) is[29]

$$A(s) = \bar{w}(s,0,t) = \sum_{n=0}^{\infty} a_n Q_n G_n(s) \frac{1}{s} \mathrm{J}_{n+1}\left(s\frac{1-b}{2}\right), \tag{27}$$

$$B(s) = \bar{\phi}(s,0,t) - \frac{e_{15}}{\varepsilon_{11}}\bar{w}(s,0,t) = \sum_{n=0}^{\infty}\left(b_n - \frac{e_{15}}{\varepsilon_{11}}a_n\right) Q_n G_n(s) \frac{1}{s} \mathrm{J}_{n+1}\left(s\frac{1-b}{2}\right), \tag{28}$$

$$Q_n = 2\sqrt{\pi}\frac{\Gamma(n+1+1/2)}{n!}, \tag{29}$$

$$G_n(s) = \begin{cases} (-1)^{\frac{n}{2}}\cos\left(s\dfrac{1+b}{2}\right) & (n = 0,2,4,6,\cdots), \\ (-1)^{\frac{n+1}{2}}\sin\left(s\dfrac{1+b}{2}\right) & (n = 1,3,5,7,\cdots), \end{cases} \tag{30}$$

where $\Gamma(x)$ and $\mathrm{J}_n(x)$ are the Gamma and Bessel functions, respectively.

Substituting Eqs. (27) and (28) into Eqs. (19) - (22), respectively, Eqs. (19) and (21) can be automatically satisfied, respectively. Then the remaining Eqs. (20) and (22) are reduced to the form after integration with respect to x in $[b, x]$, respectively.

$$\sum_{n=0}^{\infty} a_n Q_n \int_0^{\infty} s^{-1} G_n(s) \mathrm{J}_{n+1}\left(s\frac{1-b}{2}\right)\left[1+\frac{g_1(s)}{s g_2(s)}\right][\sin(sx) - \sin(sb)]\mathrm{d}s =$$

$$\frac{\pi}{2\mu}\tau_0(1+\lambda)(x-b), \tag{31}$$

$$\sum_{n=0}^{\infty}\left(b_n - \frac{e_{15}}{\varepsilon_{11}}a_n\right) Q_n \int_0^{\infty} s^{-1} G_n(s) \mathrm{J}_{n+1}\left(s\frac{1-b}{2}\right)\{1 + [F_2(s) - 1]\}\times$$

$$[\sin(sx) - \sin(sb)]\mathrm{d}s = -\frac{\pi D_0}{2\varepsilon_{11}}(x - b), \tag{32}$$

where $\lambda = \frac{e_{15} D_0}{\varepsilon_{11}\tau_0}$, $g_1(s) = (\gamma_1 - s) - (\gamma_1 + s)\mu_3\exp[-2\gamma_1 h]$,

$g_2(s) = 1 + \mu_3\exp[-2\gamma_1 h]$.

The semi-infinite integral in Eqs.(31) and (32) can be modified as[28]

$$\int_0^\infty \frac{1}{s}\mathrm{J}_{n+1}(s\frac{1-b}{2})\left[1 + \frac{g_1(s)}{sg_2(s)}\right]\cos(s\frac{1+b}{2})\sin(sx)\mathrm{d}s = \frac{1}{2(n+1)}\left\{\frac{\left(\frac{1-b}{2}\right)^{n+1}\sin\left(\frac{(n+1)\pi}{2}\right)}{\left[\left\{x + \frac{1+b}{2} + \sqrt{\left(x+\frac{1+b}{2}\right)^2 - \left(\frac{1-b}{2}\right)^2}\right\}^{n+1}\right.} - \sin\left[(n+1)\arcsin\left(\frac{1+b-2x}{1-b}\right)\right]\right\} + \int_0^\infty \frac{g_1(s)}{s^2 g_2(s)}\mathrm{J}_{n+1}(s\frac{1-b}{2})\cos(s\frac{1+b}{2})\sin(sx)\mathrm{d}s, \tag{33}$$

$$\int_0^\infty \frac{1}{s}\mathrm{J}_{n+1}(s\frac{1-b}{2})[1 + \frac{g_1(s)}{sg_2(s)}]\sin(s\frac{1+b}{2})\sin(sx)\mathrm{d}s = \frac{1}{2(n+1)}\left\{\cos[(n+1)\arcsin(\frac{1+b-2x}{1-b})] - \frac{\left(\frac{1-b}{2}\right)^{n+1}\cos\left(\frac{(n+1)\pi}{2}\right)}{\left\{x + \frac{1+b}{2} + \sqrt{\left(x+\frac{1+b}{2}\right)^2 - \left(\frac{1-b}{2}\right)^2}\right\}^{n+1}}\right\} + \int_0^\infty \frac{g_1(s)}{s^2 g_2(s)}\mathrm{J}_{n+1}(s\frac{1-b}{2})\sin(s\frac{1+b}{2})\sin(sx)\mathrm{d}s. \tag{34}$$

For a large s, the integrands of the semi-infinite integral in Eqs.(33) and (34) almost all $1/s^2$ except for the singularities in the integrands of the integrals in Eq.(33). The singularities in the integrands of the integrals that define the function $g_2(s)$ in Eq.(33) are poles that occur in the complex s-plane at the zero of $g_2(s)$. The technique merely deforms the contour of integration below the real s-axis so that no poles occur on the path of integration. These zero points of $g(s)$ not only depend on the crack length, the electric loading and the frequency of the incident wave, but also depend on the properties of the materials. The poles represent the addition of a free wave solution that will ensure that the scattering wave solution does not contain standing waves[30]. Note that the integrals in Eq.(33) will also have principal value integrals. So the semi-infinite integral in the Eqs.(33) and (34) can be evaluated numerically by Filon's method[31]. Thus the semi-infinite integral in Eqs.(31) and (32) can be evaluated directly. Eqs.(31) and (32) can now be solved for the coefficients a_n and b_n by the Schmidt's method. For brevity, Eq.(31) can be rewritten as (Eq.(32) can be solved using a similar method as follows)

$$\sum_{n=0}^{\infty} a_n E_n(x) = U(x) \qquad (b < x < 1), \tag{35}$$

where $E_n(x)$ and $U(x)$ are known functions and coefficient a_n is unknown and will be determined. A set of functions $P_n(x)$ which satisfy the orthogonality condition

$$\int_b^1 P_m(x) P_n(x)\mathrm{d}x = N_n \delta_{mm}, \qquad N_n = \int_b^1 P_n^2(x)\mathrm{d}x \tag{36}$$

can be constructed from the function, $E_n(x)$, such that

$$P_n(x) = \sum_{i=0}^{n} \frac{M_{in}}{M_{nn}} E_i(x), \tag{37}$$

where M_{ij} is the cofactor of the element d_{ij} of D_n, which is defined as

$$D_n = \begin{bmatrix} d_{00}, d_{01}, d_{02}, \cdots, d_{0n} \\ d_{10}, d_{11}, d_{12}, \cdots, d_{1n} \\ d_{20}, d_{21}, d_{22}, \cdots, d_{2n} \\ \cdots \\ \cdots \\ \cdots \\ d_{n0}, d_{n1}, d_{n2}, \cdots, d_{nn} \end{bmatrix}, \quad d_{ij} = \int_b^1 E_i(x) E_j(x)\mathrm{d}x. \tag{38}$$

Using Eqs.(35) - (38), we obtain

$$a_n = \sum_{j=n}^{\infty} q_j \frac{M_{nj}}{M_{jj}} \text{ with } q_j = \frac{1}{N_j}\int_0^1 U(x) P_j(x)\mathrm{d}x. \tag{39}$$

3 Intensity Factors

Coefficients a_n and b_n are known, so that entire perturbation stress field and the perturbation electric displacement can be obtainable. However, in fracture mechanics, it is of importance to determine the perturbation stress τ_{yz} and the perturbation electric displacement D_y in the vicinity of the crack's tips. τ_{yz} and D_y along the crack line can be expressed respectively as

$$\begin{aligned} \tau_{yz}(x,0,t) = & -\frac{2\mu}{\pi}\sum_{n=0}^{\infty} a_n Q_n \int_0^{\infty} G_n(s)\left\{1 + \left[\frac{\gamma_1}{s}F_1(s) - 1\right]\right\}\times \\ & \mathrm{J}_{n+1}\left(s\frac{1-b}{2}\right)\cos(xs)\mathrm{d}s - \frac{2e_{15}}{\pi}\sum_{n=0}^{\infty}\left(b_n - \frac{e_{15}}{\varepsilon_{11}}a_n\right) Q_n \int_0^{\infty} G_n(s) \times \\ & \{1 + [F_2(s) - 1]\}\mathrm{J}_{n+1}\left(s\frac{1-b}{2}\right)\cos(xs)\mathrm{d}s, \end{aligned} \tag{40}$$

$$\begin{aligned} D_y(x,0,t) = & \frac{2}{\pi}\sum_{n=0}^{\infty}(\varepsilon_{11} b_n - e_{15} a_n) Q_n \int_0^{\infty} G_n(s)\{1 + [F_2(s) - 1]\}\times \\ & \mathrm{J}_{n+1}\left(s\frac{1-b}{2}\right)\cos(xs)\mathrm{d}s. \end{aligned} \tag{41}$$

Observing the expression in Eqs. (40) and (41), the singular portion of the stress field and the singular portion of electric displacement can be obtained respectively from the relationships[28]:

$$\cos\left(s\,\frac{1+b}{2}\right)\cos(sx) = \frac{1}{2}\left\{\cos\left[s\left(\frac{1+b}{2}-x\right)\right] + \cos\left[s\left(\frac{1+b}{2}+x\right)\right]\right\},$$

$$\sin\left(s\,\frac{1+b}{2}\right)\cos(sx) = \frac{1}{2}\left\{\sin\left[s\left(\frac{1+b}{2}-x\right)\right] + \sin\left[s\left(\frac{1+b}{2}+x\right)\right]\right\},$$

$$\int_0^\infty \mathrm{J}_n(sa)\cos(bs)\,\mathrm{d}s = \begin{cases} \dfrac{\cos[n \arcsin(b/a)]}{\sqrt{a^2-b^2}} & (a > b), \\ -\dfrac{a^n \sin(n\pi/2)}{\sqrt{b^2-a^2}\,[b+\sqrt{b^2-a^2}]^n} & (b > a), \end{cases}$$

$$\int_0^\infty \mathrm{J}_n(sa)\sin(bs)\,\mathrm{d}s = \begin{cases} \dfrac{\sin[n \arcsin(b/a)]}{\sqrt{a^2-b^2}} & (a > b), \\ \dfrac{a^n \cos(n\pi/2)}{\sqrt{b^2-a^2}\,[b+\sqrt{b^2-a^2}]^n} & (b > a). \end{cases}$$

The singular part of the perturbation stress field and the singular part of the perturbation electric displacement can be expressed respectively as follows:

$$\tau = -\frac{1}{\pi}\sum_{n=0}^{\infty}(c_{44}a_n + e_{15}b_n)Q_n H_n(b,x), \tag{42}$$

$$D = -\frac{1}{\pi}\sum_{n=0}^{\infty}(\varepsilon_{11}b_n - e_{15}a_n)Q_n H_n(b,x), \tag{43}$$

where $H_n(b,x) = (-1)^{n+1}f_1(b,x,n) \quad (n = 0,1,2,3,4,5,\cdots \text{ (for } 0 < x < b)),$

$H_n(b,x) = -f_2(b,x,n) \quad (n = 0,1,2,3,4,5,\cdots \text{ (for } 1 < x)),$

$$f_1(b,x,n) = \frac{2(1-b)^{n+1}}{\sqrt{(1+b-2x)^2-(1-b)^2}\,[1+b-2x+\sqrt{(1+b-2x)^2-(1-b)^2}]^{n+1}}.$$

$$f_2(b,x,n) = \frac{2(1-b)^{n+1}}{\sqrt{(2x-1-b)^2-(1-b)^2}\,[2x-1-b+\sqrt{(2x-1-b)^2-(1-b)^2}]^{n+1}}.$$

At the left end of the right crack, we obtain the stress intensity factor K_L as

$$K_L = \lim_{x\to b^-}\sqrt{2\pi(b-x)}\cdot\tau = \sqrt{\frac{2}{\pi(1-b)}}\sum_{n=0}^{\infty}(-1)^n(c_{44}a_n + e_{15}b_n)Q_n. \tag{44}$$

At the right end of the right crack, we obtain the stress intensity factor K_R as

$$K_R = \lim_{x\to 1^+}\sqrt{2\pi(x-1)}\cdot\tau = \sqrt{\frac{2}{\pi(1-b)}}\sum_{n=0}^{\infty}(c_{44}a_n + e_{15}b_n)Q_n. \tag{45}$$

At the left end of the right crack, we obtain the electric displacement intensity factor D_L as

$$D_L = \lim_{x\to b^-}\sqrt{2\pi(b-x)}\cdot D = \sqrt{\frac{2}{\pi(1-b)}}\sum_{n=0}^{\infty}(-1)^n(e_{15}a_n - \varepsilon_{11}b_n)Q_n. \tag{46}$$

At the right end of the right crack, we obtain the electric displacement intensity factor D_R as

$$D_R = \lim_{x \to 1^+} \sqrt{2\pi(x-1)} \cdot D = \sqrt{\frac{2}{\pi(1-b)}} \sum_{n=0}^{\infty} (e_{15} a_n - \varepsilon_{11} b_n) Q_n . \qquad (47)$$

4 Numerical Calculations and Discussions

This section presents numerical results of several representative problems. From Refs.[32 - 36], it can be seen that the Schmidt's method is performed satisfactorily if the first ten terms of the infinite series to Eq.(35) are obtained. The solution of two collinear cracks of arbitrary length $a - b$ can easily be obtained by a simple change in the numerical values of the present paper ($a > b > 0$), i.e., it can use the results of the collinear cracks of length $1 - b/a$ and the strip width h/a in the present paper. The solution of this paper is suitable for the arbitrary length two collinear cracks in the piezoelectric layer bonded to dissimilar half space. All applications were focused on two cracked piezoelectric layer bonded to half planes. The piezoelectric layer is assumed to be the commercially available piezoelectric PZT-4 or PZT-5H, and the half planes are either aluminium or epoxy. The material constants of PZT-4 are $c_{44} = 2.56 \times 10^{10}(\mathrm{N/m^2})$, $e_{15} = 12.7(\mathrm{c/m^2})$, $\varepsilon_{11} = 64.6 \times 10^{-10}(\mathrm{c/Vm^2})$, $\rho = 7\,500\ \mathrm{kg/m^3}$, respectively. The material constants of PZT-5H are $c_{44} = 2.3 \times 10^{10}(\mathrm{N/m^2})$, $e_{15} = 17.0(\mathrm{c/m^2})$, $\varepsilon_{11} = 150.4 \times 10^{-10}(\mathrm{c/Vm^2})$, $\rho = 7\,500\ \mathrm{kg/m^3}$, respectively. The material constants of aluminium are $c_{44}^{E} = 2.65 \times 10^{10}(\mathrm{N/m^2})$ and $\rho = 2\,706\ \mathrm{kg/m^3}$. The material constants of epoxy are $c_{44}^{E} = 0.176 \times 10^{10}(\mathrm{N/m^2})$ and $\rho = 1\,600\ \mathrm{kg/m^3}$. The results of the present paper are shown in Figs. 2 - 13, respectively. From the results, the following observations are very significant:

(i) The dynamic stress intensity factors not only depend on the crack length, the width of the strip, the electric loading and the frequency of the incident wave, but also on the properties of the materials. However, the electric displacement intensity factors only depend on the crack length, the width of the strip, the electric loading and the properties of the materials.

(ii) The interaction of the two collinear cracks decrease when the distance between the two collinear cracks increases.

(iii) The stress intensity factors decrease when the width of the piezoelectric layer increases.

(iv) The stress intensity factors increase with the increasing of the electric loading for the width $h > 1.0$. However, the stress intensity factor becomes small with increasing of the electric loading for the width $h < 1.0$. This is due to the coupling between the electric and the mechanical fields. However, the electric displacement intensity factors increase with the increasing of the electric loading for any h.

(v) The dynamic stress intensity factors tend to increase with the frequency reaching a peak and then to decrease in magnitude. However, when the frequency $\omega/c_{SH} > 2.4$, the dynamic stress intensity factors tend to increase with the frequency again. This phenomenon is brought up by the free wave. Here, the free wave is created by the singularities in the integrands of the integrals in Eqs.(31) and (32).

(vi) The intensity factor K_L is larger than K_R for $\omega/c_{SH} < 1.5$. However, K_L may be smaller than K_R for $\omega/c_{SH} > 1.5$. The electric displacement intensity D_L is larger than D_R.

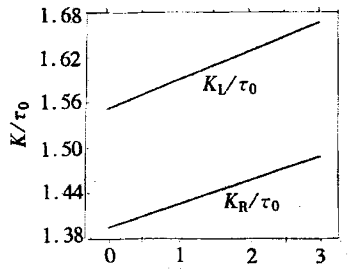

Fig.2 Stress intensity factors versus λ for $b = 0.1$, $h = 1.0$, $\omega/c_{SH} = 0.5$ (Aluminium/PZT-4/Aluminium)

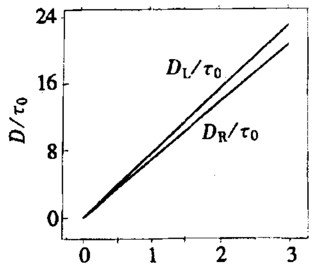

Fig.3 The electric displacement intensity factors versus λ for $b = 0.1$, $h = 1.0$, $\omega/c_{SH} = 0.5$ (Aluminium/PZT-4/Aluminium)

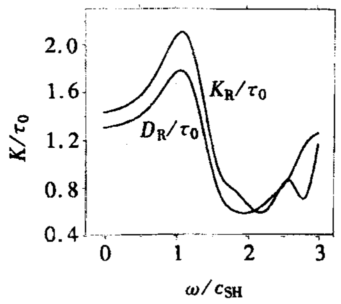

Fig.4 Stress intensity factors versus ω/c_{SH} for $b = 0.1$, $\lambda = 0.2$, $h = 1.0$ (Aluminium/PZT-4/Aluminium)

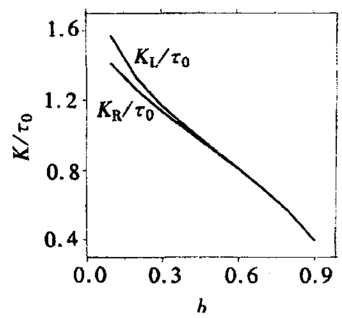

Fig.5 Stress intensity factors versus b for $\lambda = 0.5$, $h = 1.0$, $\omega/c_{SH} = 0.5$ (Aluminium/PZT-4/Aluminium)

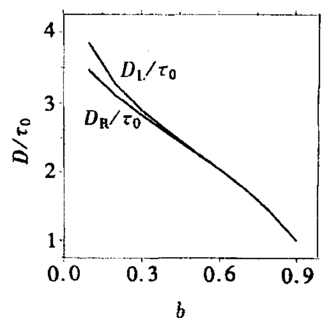

Fig.6 The electric displacement intensity factors versus b for $\lambda = 0.5$, $h = 1.0$, $\omega/c_{SH} = 0.5$ (Aluminium/PZT-4/Aluminium)

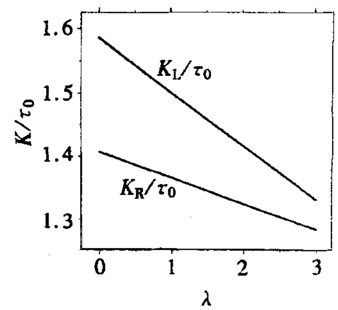

Fig.7 Stress intensity factors versus λ for $b = 0.1$, $h = 0.5$, $\omega/c_{SH} = 0.5$ (Aluminium/PZT-4/Aluminium)

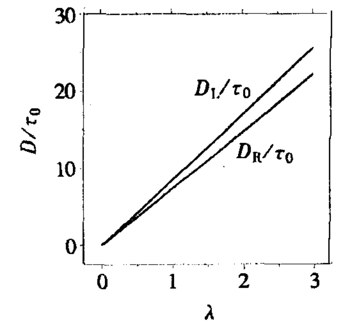

Fig.8 The electric displacement intensity factors versus λ for $b = 0.1$, $h = 0.5$, $\omega/c_{SH} = 0.5$ (Aluminium/PZT-4/Aluminium)

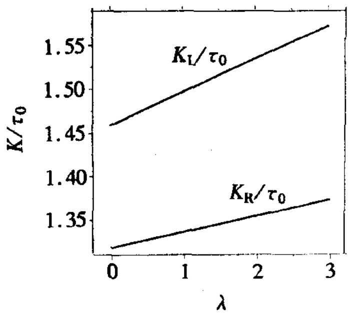

Fig.9 Stress intensity factors versus λ for $b = 0.1$, $h = 3.5$, $\omega/c_{SH} = 0.5$ (Aluminium/PZT-4/Aluminium)

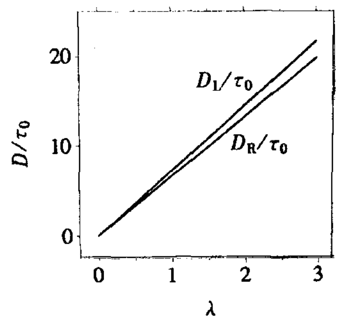

Fig.10 The electric displacement intensity factors versus λ for $b = 0.1$, $h = 3.5$, $\omega/c_{SH} = 0.5$ (Aluminium/PZT-4/Aluminium)

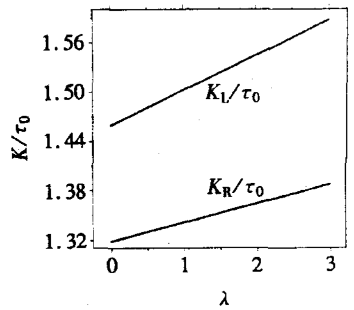

Fig.11 Stress intensity factors versus λ for $b = 0.1$, $h = 5.0$, $\omega/c_{SH} = 0.5$ (Aluminium/PZT-5H/Aluminium)

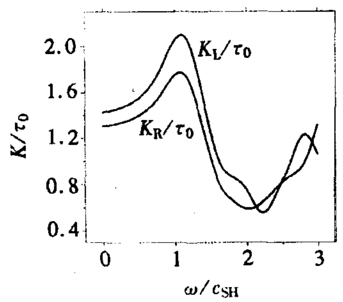

Fig.12 Stress intensity factors versus ω/c_{SH} for $b = 0.1$, $\lambda = 0.2$, $h = 1.0$ (Aluminium/PZT-5H/Aluminium)

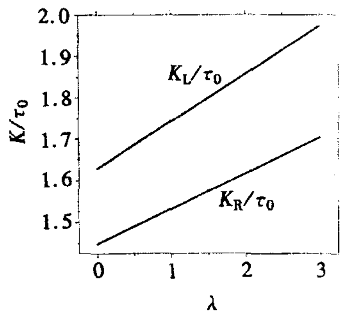

Fig.13 Stress intensity factors versus λ for $b = 0.1$, $h = 1.0$, $\omega/c_{SH} = 0.5$ (Epoxy/PZT-5H/Epoxy)

References:

[1] Deeg W E F. The analysis of dislocation, crack and inclusion problems in piezoelectric solids[D]. Ph D thesis, Stanford University, 1980.

[2] Pak Y E. Crack extension force in a piezoelectric material[J]. *Journal of Applied Mechanics*, 1990, **57**(4):647 - 653.

[3] Pak Y E. Linear electro-elastic fracture Mechanics of piezoelectric materials[J]. *International Journal of Fracture*, 1992, **54**(1):79 - 100.

[4] Sosa H A, Pak Y E. Three-dimensional eigenfunction analysis of a crack in a piezoelectric ceramics [J]. *International Journal of Solids and Structures*, 1990, **26**(1):1 - 15.

[5] Sosa H A. Plane problems in piezoelectric media with defects[J]. *International Journal of Solids and Structures*, 1991, **28**(4):491 - 505.

[6] Sosa H A. On the fracture mechanics of piezoelectric solids[J]. *International Journal of Solids and Structures*, 1992, **29**(8):2613 - 2622.

[7] Suo Z, Kuo C M, Barnett D M, *et al*. Fracture mechanics for piezoelectric ceramics[J]. *Journal of Mechanics and Physics of Solids*, 1992, **40**(5):739 - 765.

[8] Park S B, Sun C T. Fracture criteria for piezoelectric ceramics[J]. *Journal of American Ceramics Society*, 1995,**78**(7):1475 - 1480.

[9] Zhang T Y, Tong P. Fracture mechanics for a mode Ⅲ crack in a piezoelectric material[J]. *International Journal of Solids and Structures*, 1996, **33**(5):343 - 359.

[10] Gao H, Zhang T Y, Tong P. Local and global energy rates for an elastically yielded crack in piezoelectric ceramics[J]. *Journal of Mechanics and Physics of Solids*, 1997, **45**(4):491 - 510.

[11] WANG Biao. Three dimensional analysis of a flat elliptical crack in a piezoelectric materials[J]. *International Journal of Enginerring*, 1992, **30**(6): 781 - 791.

[12] Narita K, Shindo Y. Scattering of Love waves by a surface-breaking crack in piezoelectric layered media[J]. *JSME International Journal, Series A*, 1998, **41**(1): 40 - 52.

[13] Narita K, Shindo Y. Scattering of anti-plane shear waves by a finite crack in piezoelectric laminates [J]. *Acta Mechanica*, 1999, **134**(1):27 - 43.

[14] ZHOU Zhen-gong, WANG Biao, CAO Mao-sheng. Analysis of two collinear cracks in a piezoelectric layer bonded to dissimilar half spaces subjected to anti-plane shear[J]. *European Journal of Mechanics A/Solids*, 2001,**20**(2):213 - 226.

[15] YU Shou-wen, CHEN Zeng-tiao. Transient response of a cracked infinite piezoelectric strip under anti-plane impact [J]. *Fatigue and Engineering Materials and Structures*, 1998, **21** (4): 1381 - 1388.

[16] CHEN Zeng-tiao, Karihaloo B L. Dynamic response of a cracked piezoelectric ceramic under arbitrary electro-mechanical impact[J]. *International Journal of Solids and Structures*, 1999, **36**(5): 5125 - 5133.

[17] Paul H S, Nelson V K. Axisymmetric vibration of piezo-composite hollow circular cylinder[J]. *Acta Mechanica*, 1996, **116**(5):213 - 222.

[18] Khutoryansky N M, Sosa H. Dynamic representation formulas and fundamental solutions for piezoelectricity[J]. *International Journal of Solids and Structures*, 1995, **32**(8): 3307 - 3325.

[19] Shindo Y, Katsura H, Yan W. Dynamic stress intensity factor of a cracked dielectric medium in a uniform electric field[J]. *Acta Mechanica*, 1996, **117**(1): 1 - 10.

[20] Narita K, Shindo Y, Watanabe K. Anti-plane shear crack in a piezoelectric layered to dissimilar half spaces[J]. *JSME International Journal, Series A*, 1999, **42**(1): 66 - 72.

[21] Tauchert T R. Cylindrical bending of hybrid laminates under thermo-electro-mechanical loading[J]. *Journal of Thermal Stresses*, 1996, **19**(4): 287 - 296.

[22] Lee J S, Jiang L Z. Exact electro-elastic analysis of piezoelectric laminate via state space approach [J]. *International Journal of Solids and Structures*, 1996, **33**(4): 977 - 985.

[23] Tang Y Y, Noor A K, Xu K. Assessment of computational models for thermoelectroelastic multilayered plates[J]. *Computers and Structures*, 1996, **61**(6): 915 - 924.

[24] Batra R C, Liang X Q. The vibration of a rectangular laminated elastic plate with embedded piezoelectric sensors and actuators[J]. *Computer and Structures*, 1997, **63**(4):203 - 212.

[25] Heyliger P. Exact solutions for simply supported laminated piezoelectric plates[J]. *ASME Journal of Applied Mechanics*, 1997, **64**(4): 299 - 313.

[26] Shindo Y, Domon W, Narita F. Dynamic bending of a symmetric piezoelectric laminated plate with a through crack[J]. *Theoretical and Applied Fracture Mechanics*, 1998, **28**(2):175 - 184.

[27] Morse P M, Feshbach H. *Methods of Theoretical Physics*[M]. Vol 1. New York: McGraw-Hill, 1958, 828 - 929.

[28] Gradshteyn I S, Ryzhik I M. *Table of Integral, Series and Products*[M]. New York: Academic Press, 1980, 980 - 997.

[29] Erdelyi A. *Tables of Integral Transforms*[M]. Vol 1. New York: McGraw-Hill, 1954, 38 - 95.

[30] Keer L M, Luong W C. Diffraction of waves and stress intensity factors in a cracked layered composite[J]. *Journal of the Acoustical Society of America*, 1974, **56**(5): 1681 - 1686.

[31] Amemiya A, Taguchi T. *Numerical Analysis and Fortran*[M]. Tokyo: Maruzen, 1969.

[32] Itou S. Three dimensional waves propagation in a cracked elastic solid[J]. *ASME Journal of Applied Mechanics*, 1978, **45**(2): 807 - 811.

[33] Itou S. Three dimensional problem of a running crack[J]. *International Journal of Engineering Science*, 1979, **17**(7): 59 - 71.

[34] ZHOU Zheng-gong, HAN Jie-cai, DU Shan-yi. Two collinear Griffith cracks subjected to uniform tension in infinitely long strip[J]. *International Journal of Solids and Structures*, 1999, **36**(4): 5597 - 5609.

[35] ZHOU Zhen-gong, HAN Jie-cai, DU Shan-yi. Investigation of a Griffith crack subject to anti-plane shear by using the non-local theory[J]. *International Journal of Solids and Structures*, 1999, **36**(3): 3891 - 3901.

[36] ZHOU Zhen-gong, WANG Biao. Investigation of a Griffith crack subjected to uniform tension using the non-local theory by a new method[J]. *Applied Mathematics and Mechanics (English Edition)*, 1999, **20**(10): 1099 - 1107.